

# Accessing nucleonic structure with early CLAS12 results

Timothy B. Hayward

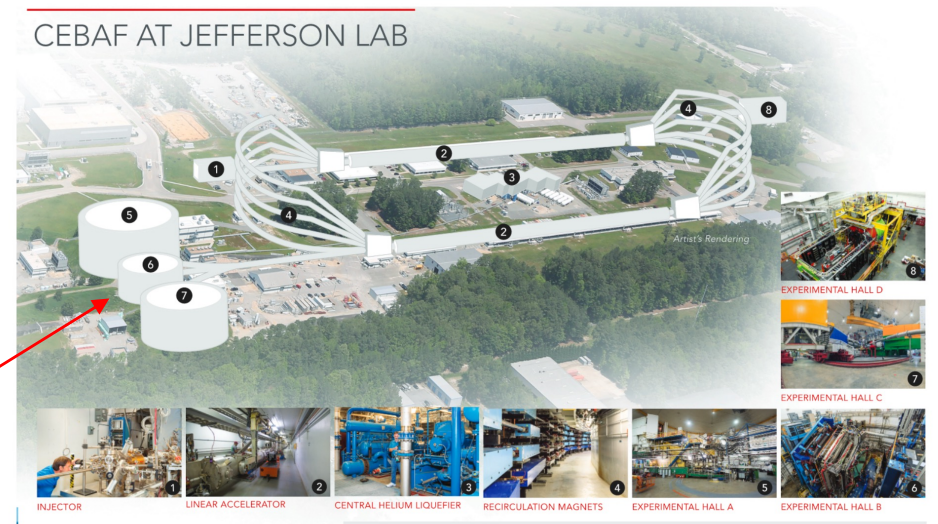


August 31, 2022

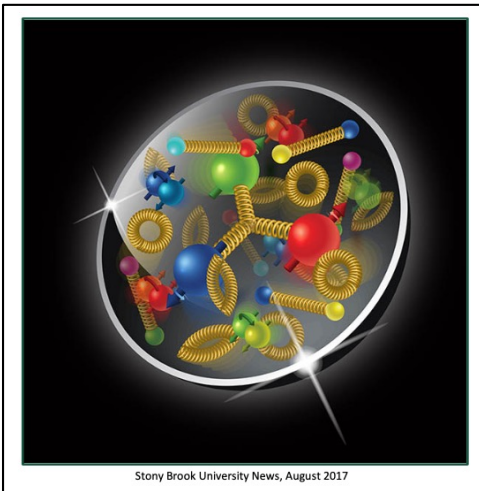
UCONN

# Thomas Jefferson National Accelerator Facility

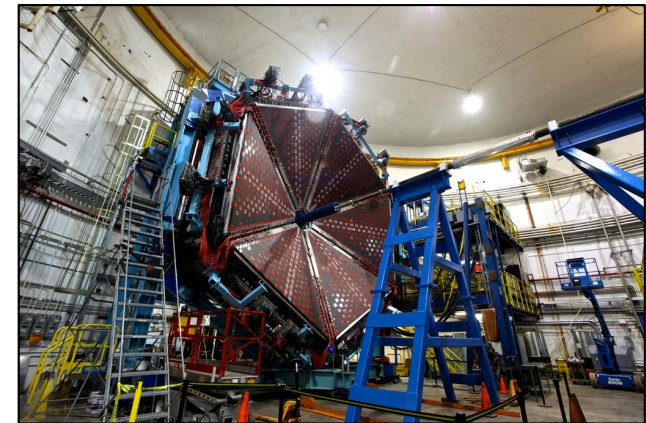
- Continuous Electron Beam Accelerator Facility (CEBAF) is located in Newport News, VA.
- Four experimental halls (A, B, C and D) receive a recently upgraded 12 GeV electron beam.
- Race track design with parallel north and south linear accelerators that pass the beam up to five times.
- CLAS12 located in Hall B.



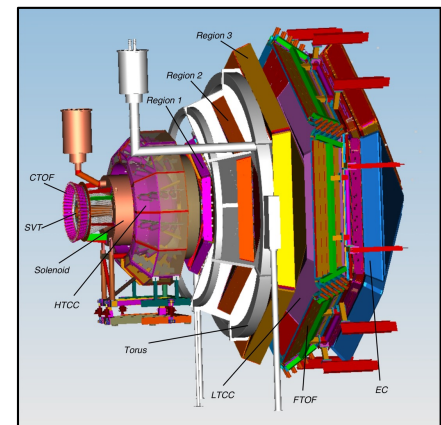
# CLAS12 (Hall B) Physics Program



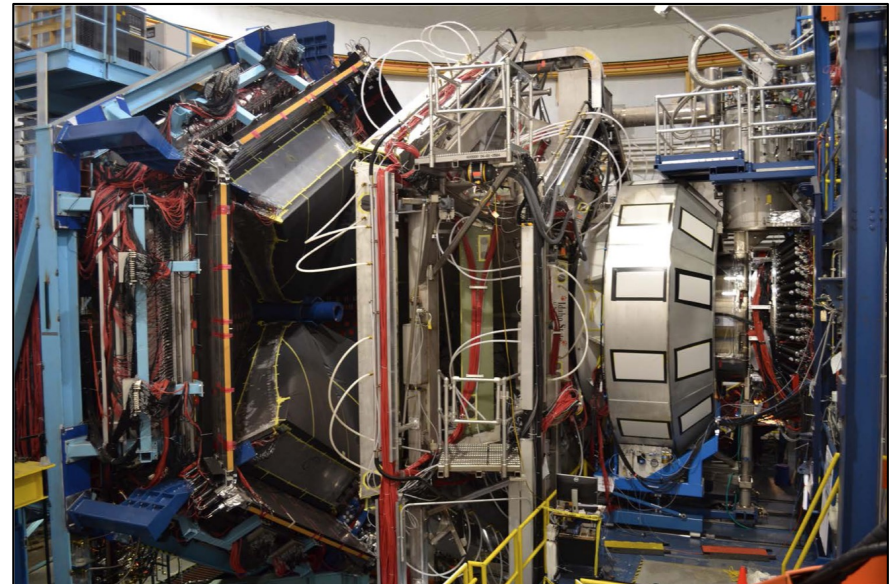
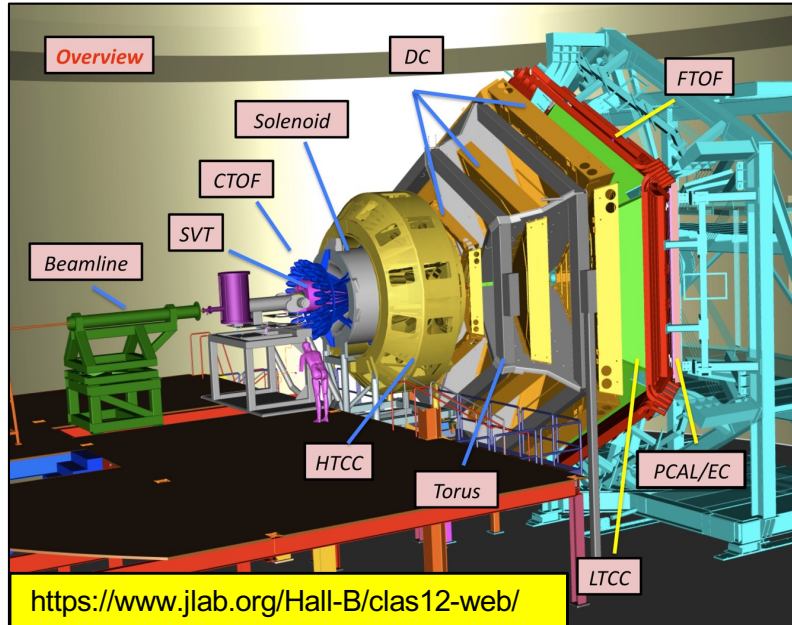
- International collaboration with more than 40 member institutions and 200 full members.
- CLAS(12) is the world's only large acceptance and high luminosity spectrometer for fixed target lepton scattering experiments.



1. Study of the nucleon resonance structure at photon virtualities from 2.0 to 12  $\text{GeV}^2$
2. Study of Generalized Parton Distributions (GPDs), (2 +1) D imaging of the proton and the study of its gravitational and mechanical structure.
3. Study of the Transverse Momentum Dependence (TMDs) and the of 3D structure in momentum space.
4. Study of J/ $\psi$  Photoproduction, LHCb Pentaquarks and Timelike Compton Scattering.
5. Study of meson spectroscopy in search of hybrid mesons
6. Much more!



# CLAS12 Spectrometer

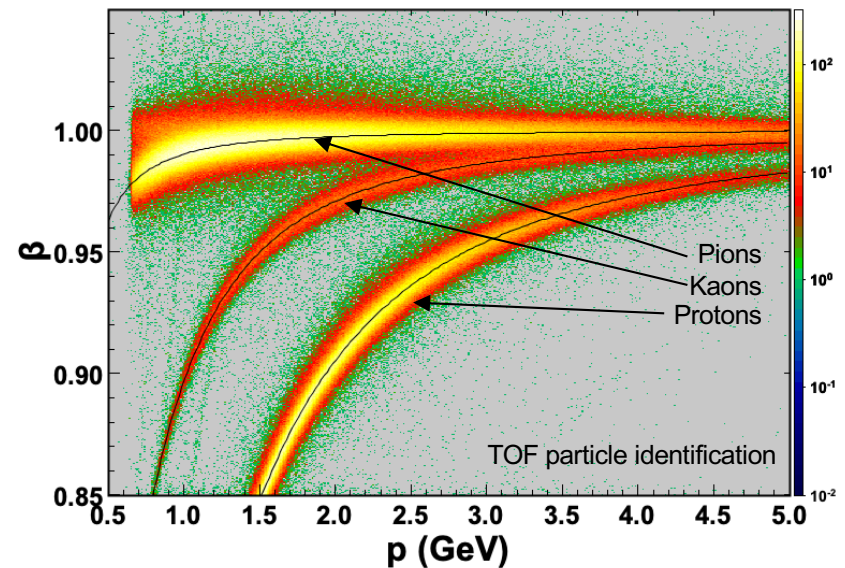
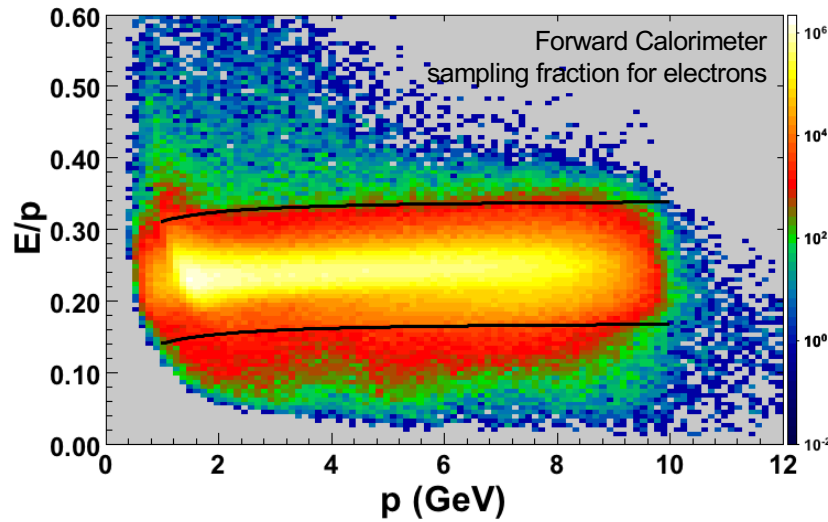


V. Burkert et al., Nucl. Instrum. Meth. A 959 (2020) 163419

- CLAS12: very high luminosity, wide acceptance, low  $Q^2$  (higher twist measurements)
- Began data taking in Spring 2018 – many “run periods” now available.
- Data from Fall 2018 (Spring 2019) - 10.6 (10.2) GeV electron beam, longitudinally polarized beam, liquid  $H_2$  target.

# Particle ID

- Electron
  - Electromagnetic calorimeter.
  - Cherenkov detector.
  - Vertex and fiducial cuts.
- Charged Hadron
  - $\beta$  vs  $p$  comparison between vertex timing and event start time.
  - 100 ps TOF resolution.
  - Vertex and fiducial cuts.



# A Constructivist View of the Nucleon

Wigner distributions

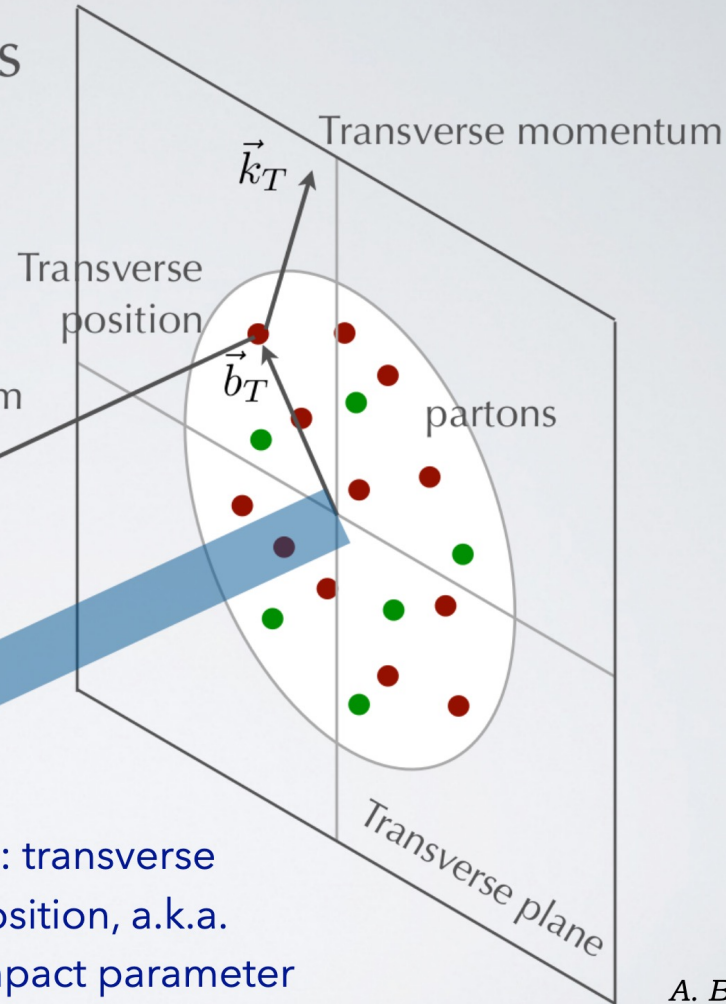
$$\rho(x, \vec{k}_T, \vec{b}_T)$$

*"phase space" distributions  
of partons in a nucleon*

Longitudinal momentum

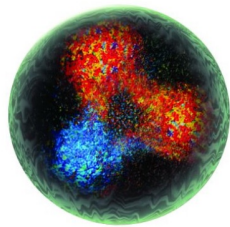
$$k^+ = xP^+$$

$x$ : longitudinal  
momentum  
fraction carried  
by struck parton



A. Bacchetta

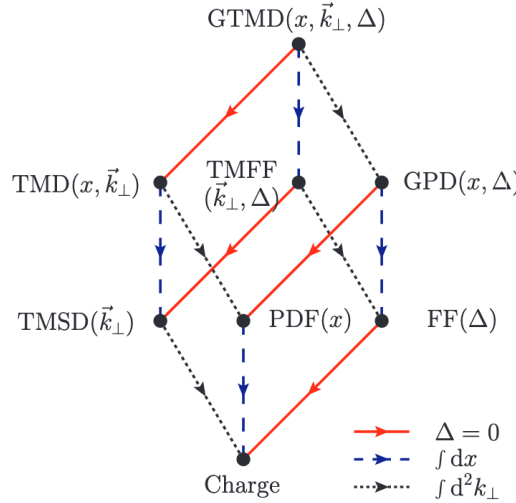
# Generalized Parton Distributions



Wigner Function,  $\rho(x, \vec{k}_T, \vec{b}_T)$ :  
Full phase space parton distribution of the nucleon

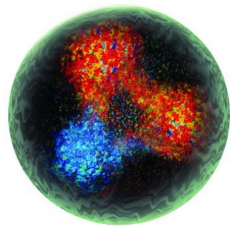


Generalized Transverse Momentum Distributions



C. Lorce et al., JHEP 05, 041, (2011), [hep-ph] 1102.4704

# Generalized Parton Distributions



**Wigner Function,  $\rho(x, \vec{k}_T, \vec{b}_T)$ :**  
Full phase space parton distribution of the nucleon



Generalized Transverse Momentum Distributions

Generalized Parton Distributions

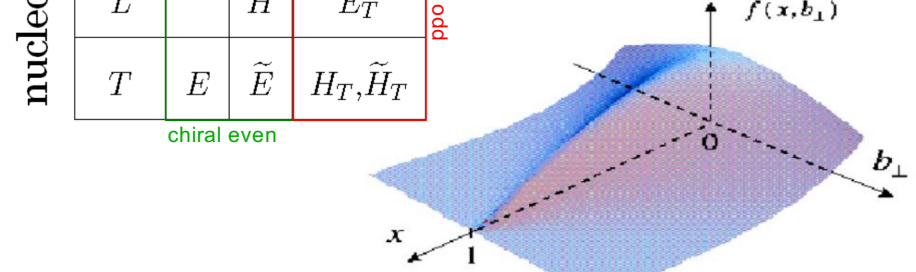
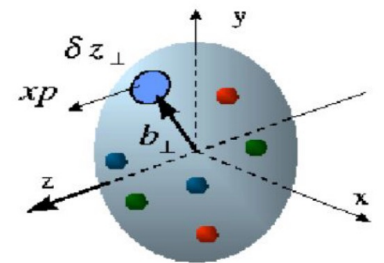
- Relate the transverse position of partons to the longitudinal momentum
- Measured in: deep exclusive reactions (DVCS, DVMP, TCS, etc.)

| N/q | U | L           | T                  |
|-----|---|-------------|--------------------|
| U   | H |             | $\bar{E}_T$        |
| L   |   | $\tilde{H}$ | $\tilde{E}_T$      |
| T   | E | $\tilde{E}$ | $H_T, \tilde{H}_T$ |

quark pol.

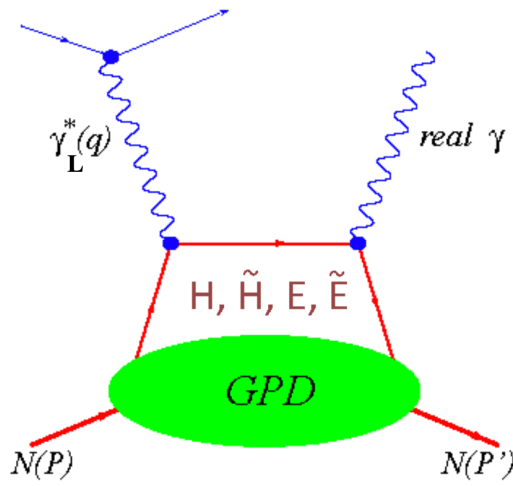
nucleon pol.

chiral even      chiral odd



# DVCS and TCS

## Deeply Virtual Compton Scattering (DVCS)



- + Clean process
- Only sensitive to chiral even GPDs

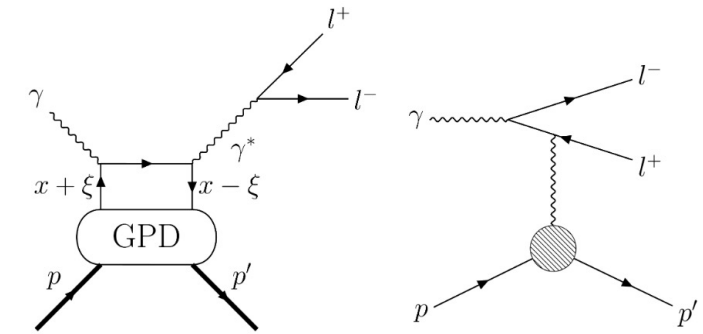
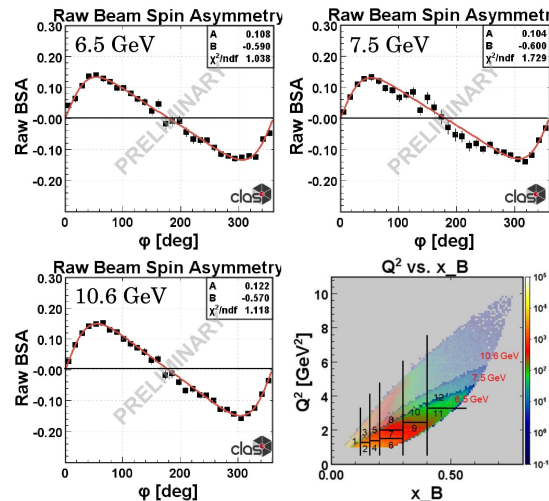
DVCS

BH

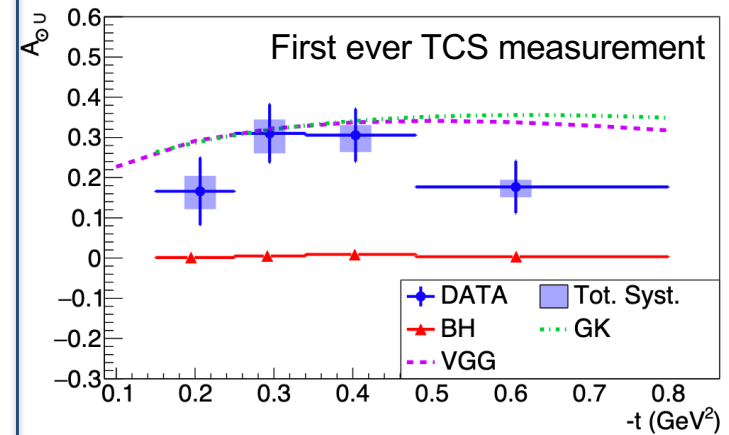
$$\mathcal{M}^2 = |\mathcal{M}_{\text{DVCS}} + \mathcal{M}_{\text{BH}}|^2 = |\mathcal{M}_{\text{DVCS}}|^2 + |\mathcal{M}_{\text{BH}}|^2 + \mathcal{I}$$

- Normal strategy to measure the interference term.
- With multiple measurements at different energies, we can perform a Rosenbluth separation to access things like the shear and pressure of the nucleon through the CFFs.

$$A_{LU} \propto F_1 \mathcal{H} + \xi G_M \tilde{\mathcal{H}} - \frac{t}{4M^2} F_2 \mathcal{E}$$



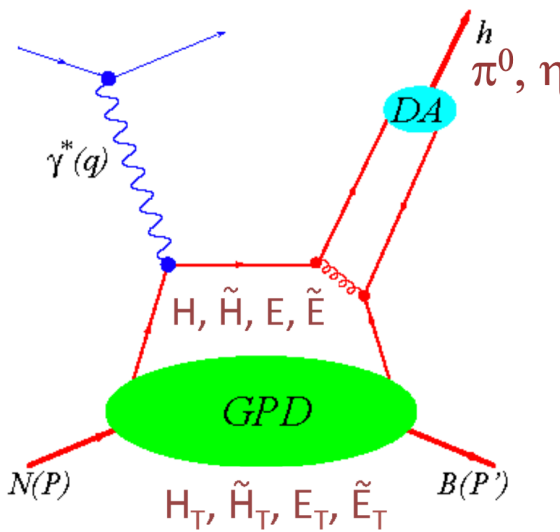
(Timelike) Compton Scattering is the time reversal process of DVCS and allows us to test the universality of GPDs.



P. Chatagnon et al., Phys. Rev. Lett., 127, 262501, (2021), [hep-ex] 2108.11746

# Deeply Virtual Meson Production

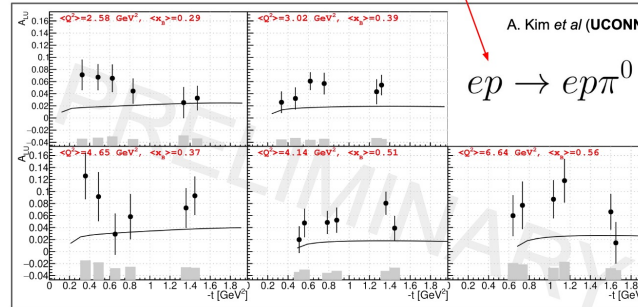
## Deeply Virtual Meson Production (DVMP)



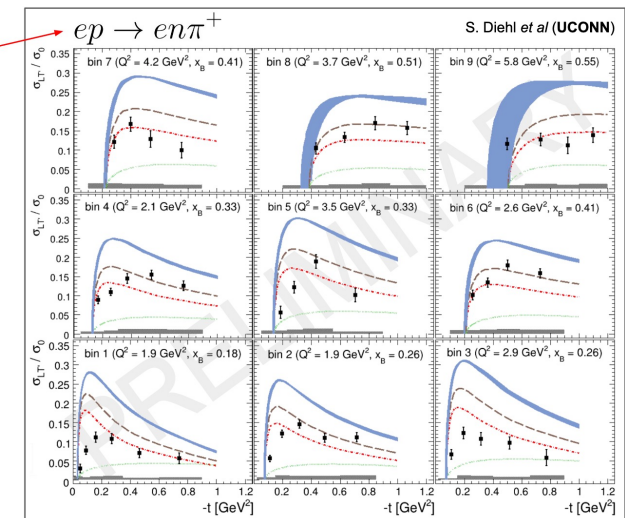
- + Enables Flavour decomposition of GPDs
- + Access to transversity degrees of freedom described by chiral-odd GPDs
- Distribution Amplitude (DA) is involved as additional soft non pert. quantity

| Meson    | Flavor                 |
|----------|------------------------|
| $\pi^+$  | $\Delta u - \Delta d$  |
| $\pi^0$  | $2\Delta u + \Delta d$ |
| $\eta$   |                        |
| $\rho^+$ | $u - d$                |
| $\rho^0$ |                        |
| $\omega$ |                        |
| $\phi$   |                        |
| $g$      |                        |

$$\sigma_{LT'} = \xi \sqrt{1 - \xi^2} \frac{\sqrt{-t'}}{2m} \times \text{Im} [\langle H_T \rangle^* \langle \tilde{E} \rangle + \langle \bar{E}_T \rangle^* \langle \tilde{H} \rangle]$$

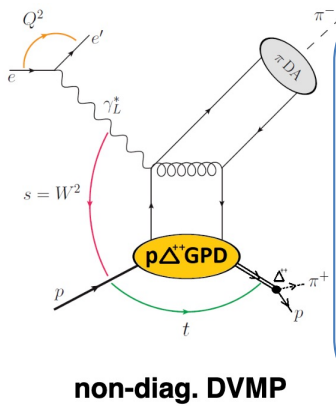
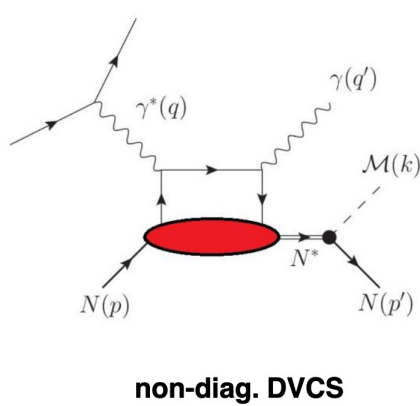


- DVMP offers access to the chiral odd GPDs with separate pseudoscalar and vector meson measurements providing information on the flavor dependence.
- Chiral odd GPDs provide access to information on proton anomalous tensor magnetic moment, proton tensor charge and more.

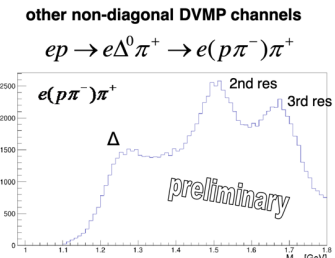
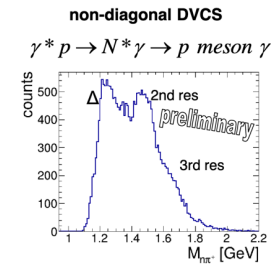
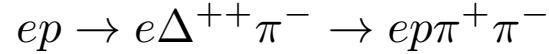


Ongoing CLAS12 analysis of  $\pi^0, \pi^+, \eta, \rho, \omega, \phi, N \rightarrow \Delta$  transition GPDs...

# Transition GPDs

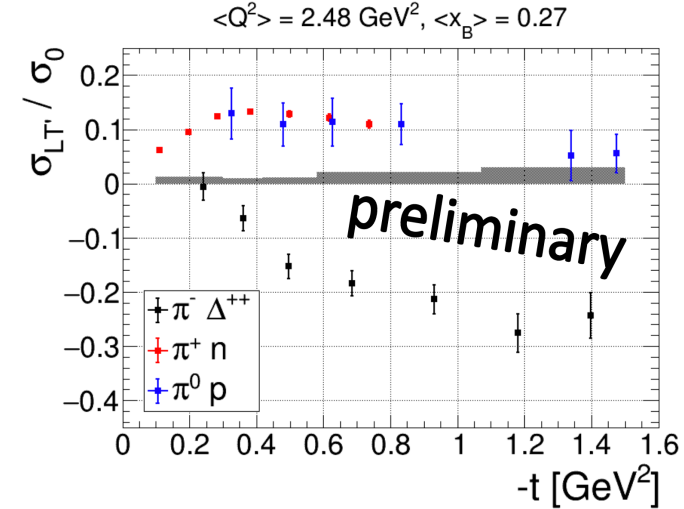
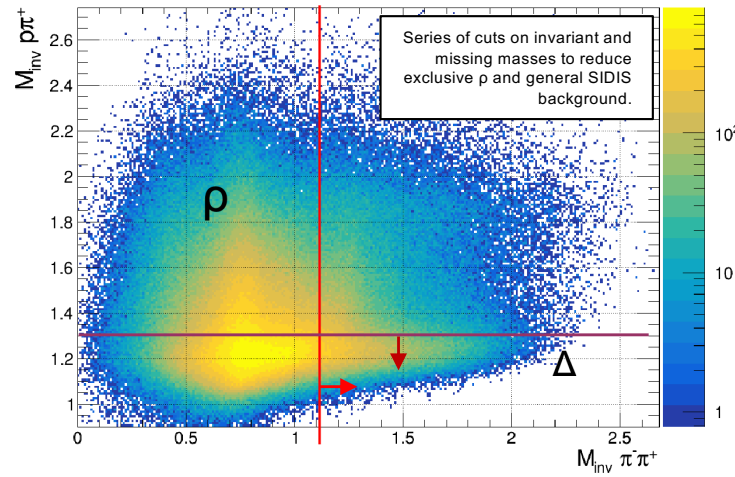


- The doubly positive  $p\pi^+$  final state can **only** be populated by  $\Delta$ -resonances.
- Large gap between  $\Delta(1232)$  and the higher resonances.
- The required constraints on  $-t$  and detection of many final state particles makes CLAS12 and ideal place to study transition GPDs.



**Factorization expected for:**  
 $-t / Q^2 \ll 1$  and  $Q^2 > M_\Delta^2$   
 $x_B$  fixed

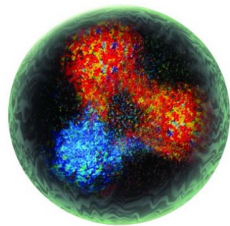
- Provides access to  $p\Delta$  transition GPDs
- 3D structure of the  $\Delta$  resonance and of the excitation process
- $\pi^\pm$  is expected to be especially sensitive to the tensor charge of the resonance



- Clearly negative asymmetry (consequence of d-quark?) with magnitude larger than exclusive  $\pi^+$ .
- First “clean” access to  $p\Delta$  transition GPDs.

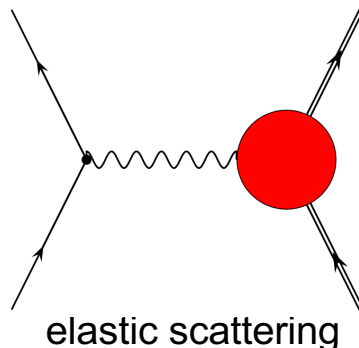
# Form Factors

Wigner Function,  $\rho(x, \vec{k}_T, \vec{b}_T)$ :  
Full phase space parton distribution of the nucleon



Generalized Transverse Momentum Distributions

Generalized Parton Distributions

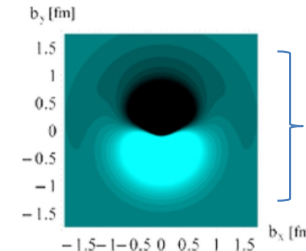
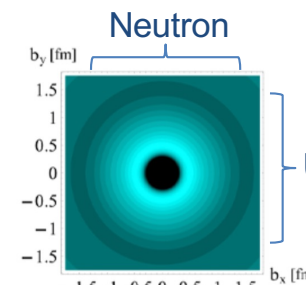
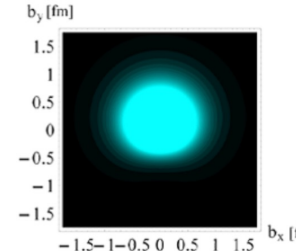
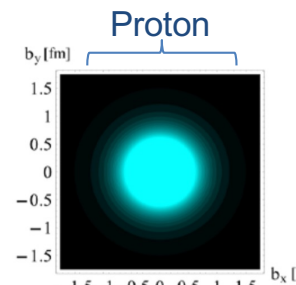


elastic scattering

$$\int d^2 k_T$$

$$\int dx$$

Form Factors

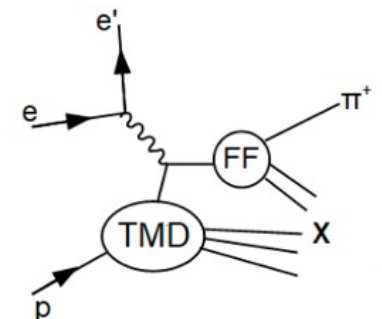
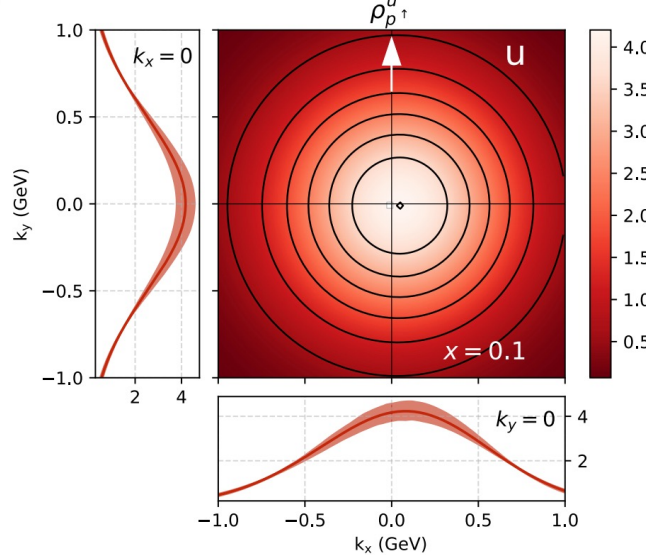
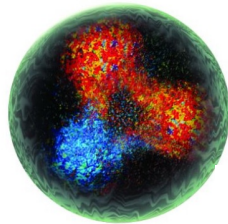


Unpolarized

Polarized

C. E. Carlson and M. Vanderhaegen, Eur.Phys.J.A 41, (2009), [hep-ph] 0807.4537

# Transverse Momentum Distributions



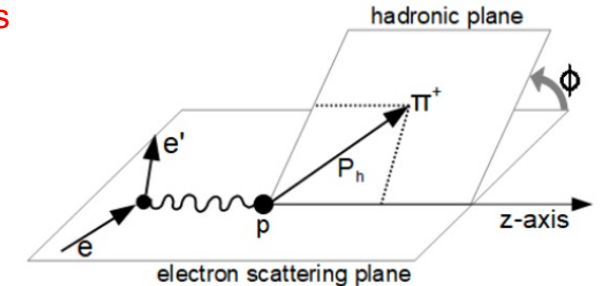
# Single Hadron Production

$$F_{LU}^{\sin \phi_h} = \frac{2M}{Q} C \left[ -\frac{\hat{h} \cdot k_T}{M_h} \left( xe H_1^\perp + \frac{M_h}{M} f_1 \tilde{G}^\perp \right) + \frac{\hat{h} \cdot p_T}{M} \left( x g^\perp D_1 + \frac{M_h}{M} h_1^\perp \tilde{E} \right) \right]$$

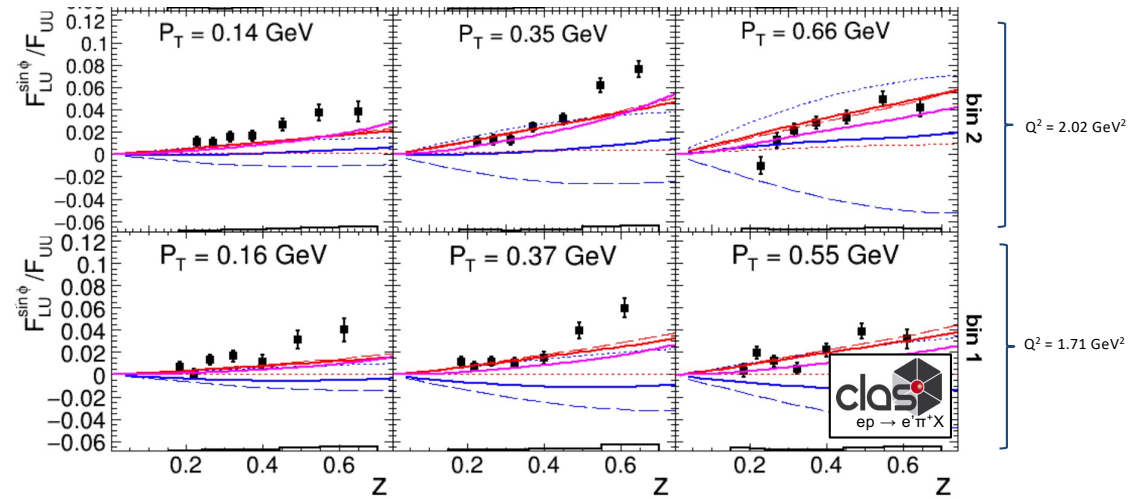
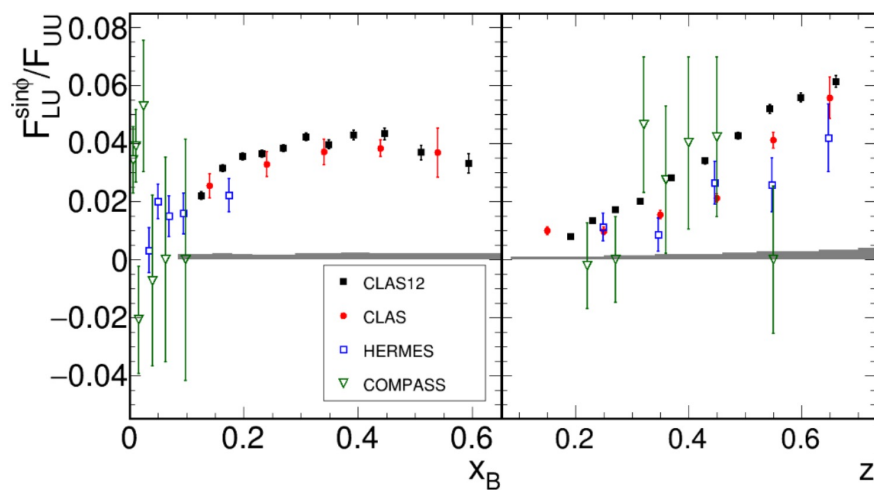
Collins FF      twist-3 FF      unpolarized FF      twist-3 FF

twist-3 pdf      unpolarized PDF      twist-3 t-odd PDF      Boer-Mulders

A. Bacchetta et al., JHEP 0702, 093 (2007).

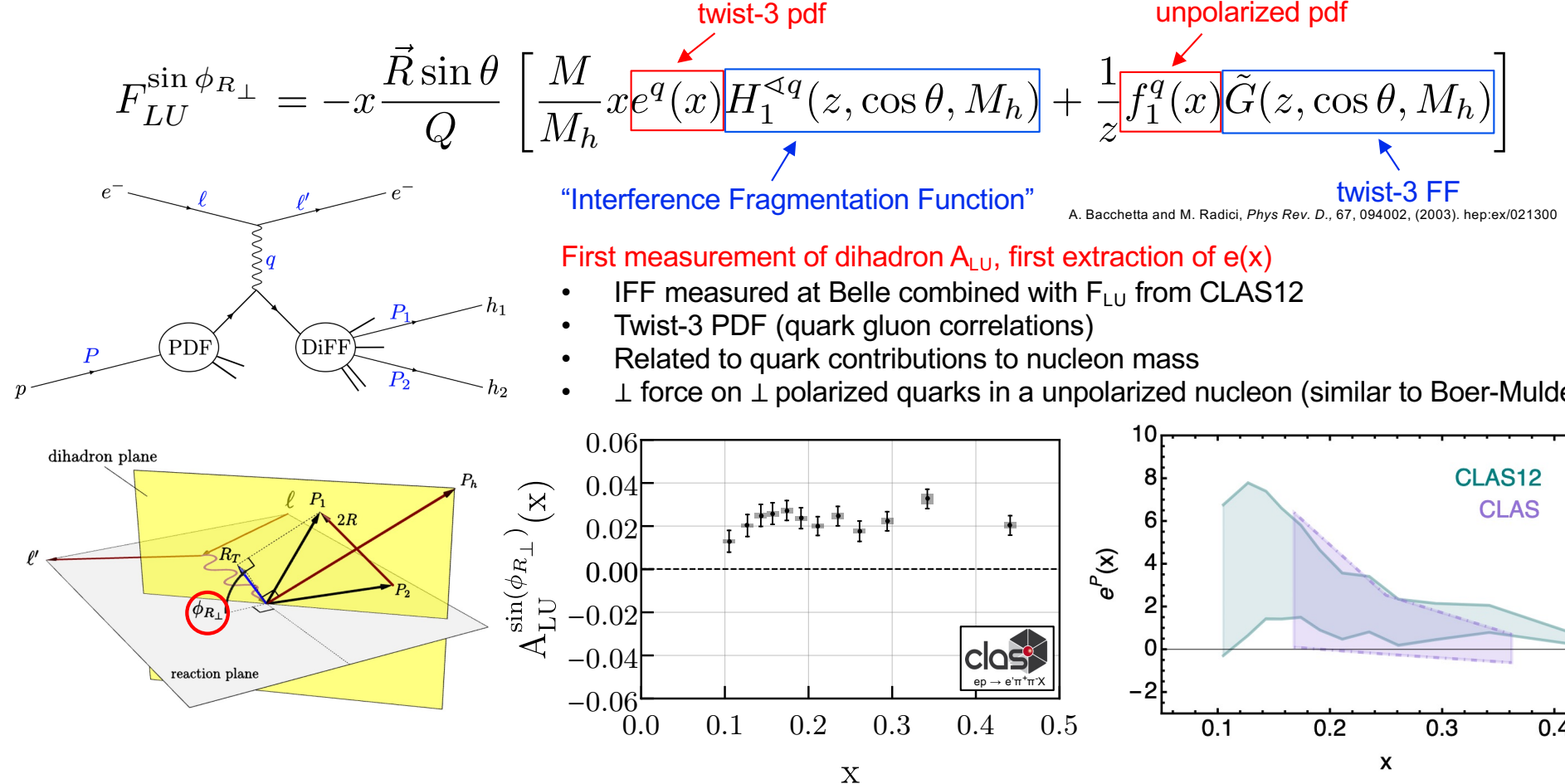


First high-precision multidimensional study: important for constraints of PDFs.

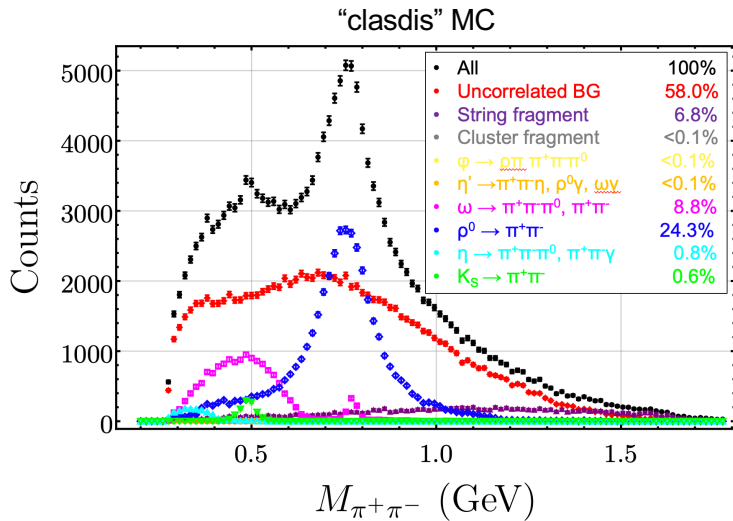


S. Diehl et al., Phys. Rev. Lett., 128, 062005, (2022), [hep-ex] 2101.03544

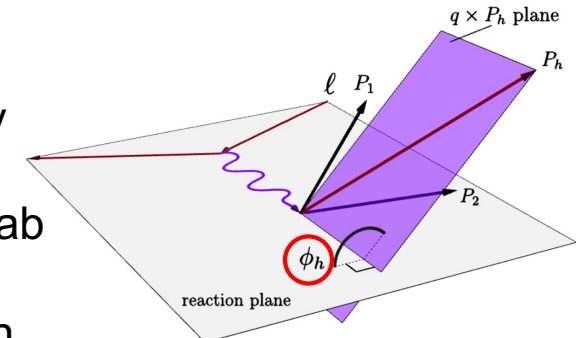
# Collinear Dihadron Production



# Vector Meson Contributions

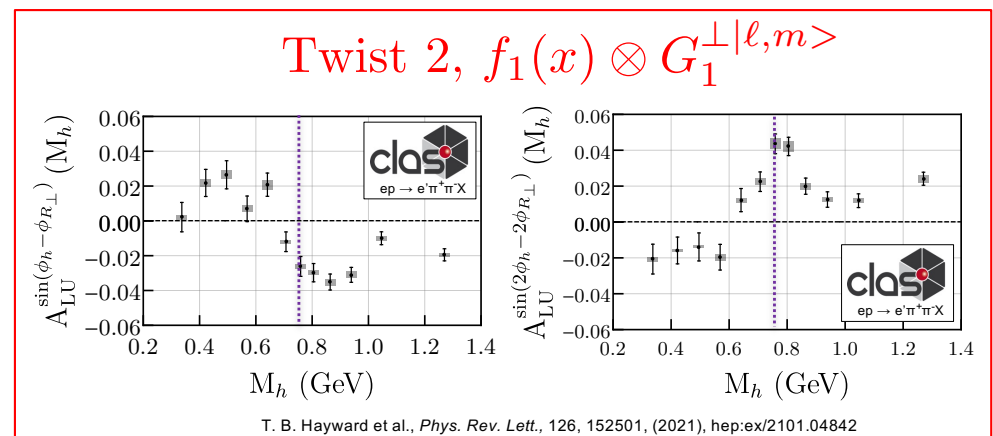


- Spin-azimuthal correlations in hadron pair production are very significant.
- Hadron pairs in SIDIS (from JLab to LHC) are dominated by VM decays (therefore single hadron channel too).



$$G_1^\perp = \frac{h_1}{h_2} - \frac{h_2}{h_1}$$

- Dihadron studies allow for the existence of FFs with no single hadron analog.
- $G_1^\perp$  describes the azimuthal dependence of an unpolarized hadron pair on the helicity of the struck quark.
- **First ever observation.**



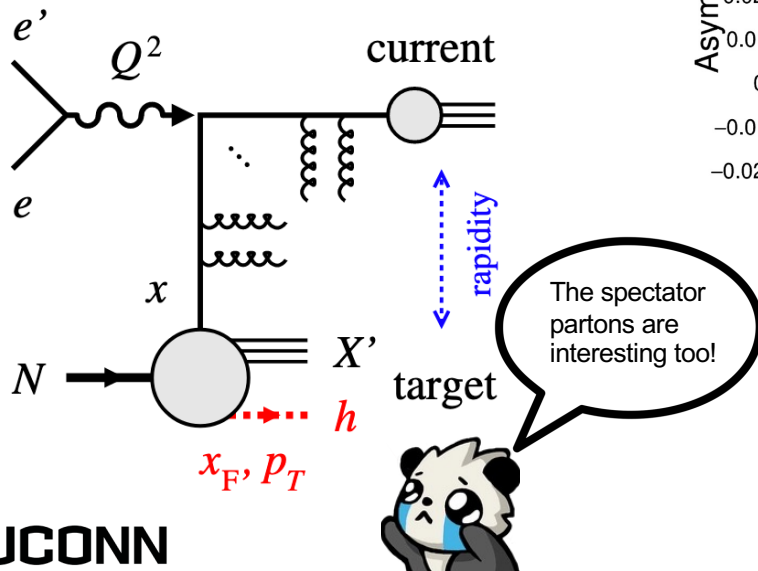
# Fracture Functions

In addition to the CFR, hadrons also form from the left-over target remnant (TFR) whose partonic structure is defined by “fracture functions”<sup>1,2</sup>: the probability for the target remnant to form a certain hadron given a particular ejected quark.

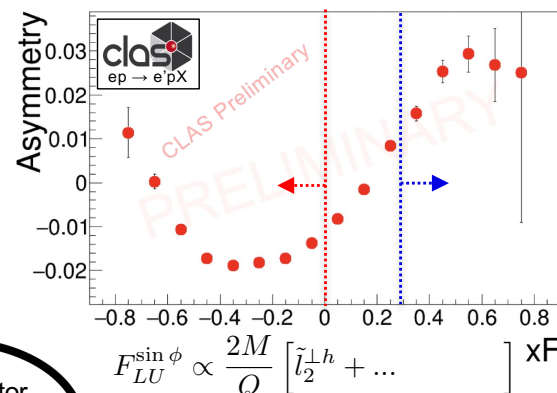
$$\frac{d\sigma^{\text{TFR}}}{dx_B dy dz} = \sum_a e_a^2 (1 - x_B) M_a(x_B, (1 - x_B)z) \frac{d\hat{\sigma}}{dy}$$

1. L. Trentadue and G. Veneziano, Phys. Lett. B323 (1994) 201,
2. M. Anselmino et al., Phys. Lett. B. 699 (2011), 108-118, [hep-ph] 1102.4214

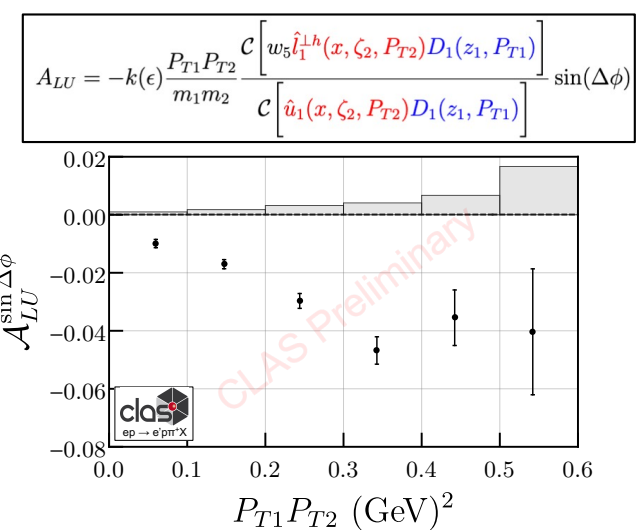
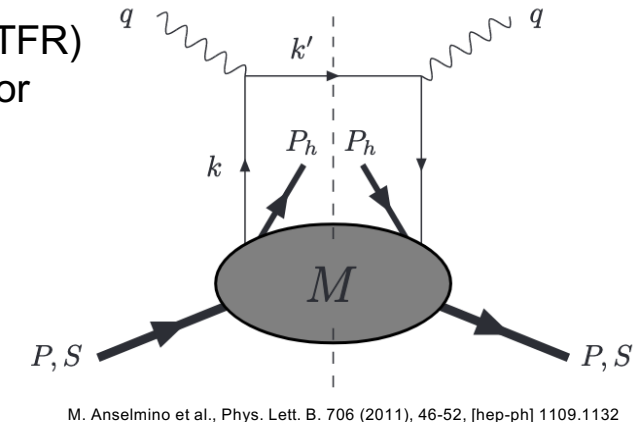
TFR/CFR Fig. from EIC Yellow Report, (2021) [physics.ins-det] 2103.05419



UCONN

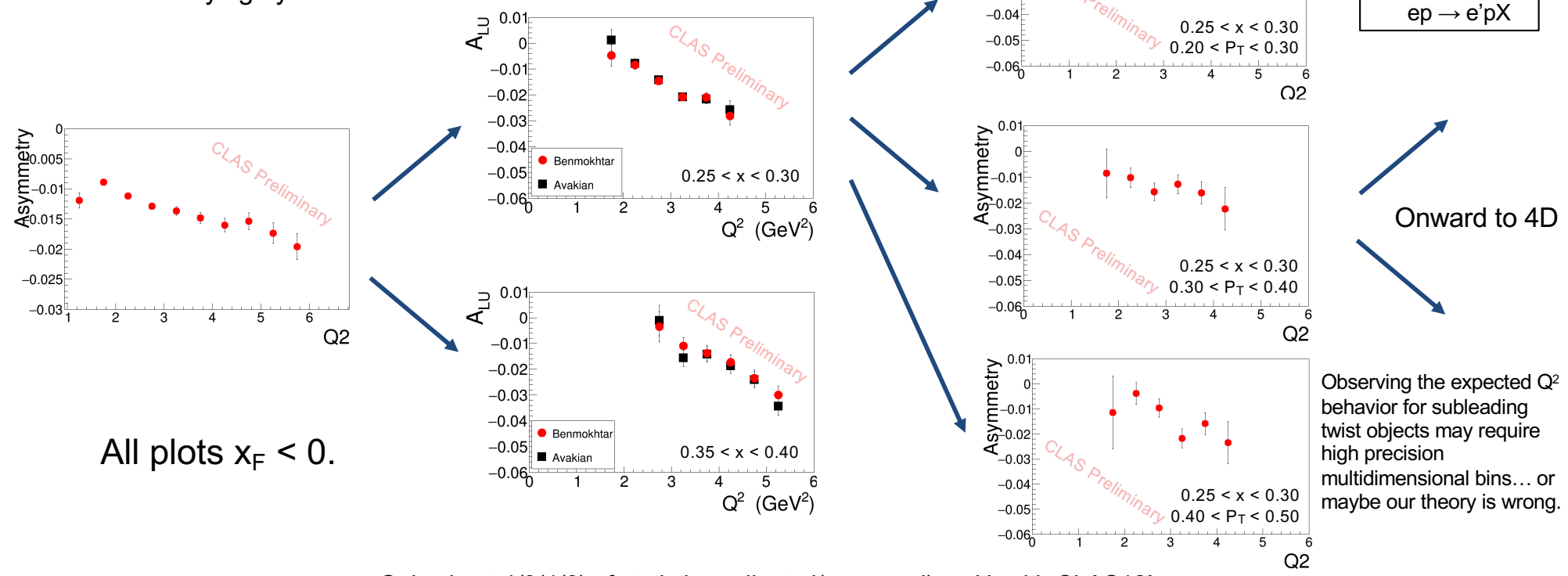


First ever observation of TMD fracture functions.

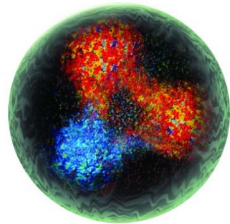


# Mapping the $Q^2$ dependence

- SSAs in single hadron production are twist-3 (M/Q suppression).
- "Twist 3" asymmetries not behaving as expected at EMC, COMPASS, CLAS12, etc.
- Proper interpretation of the  $Q^2$  dependence is crucial for our understanding of the underlying dynamics.

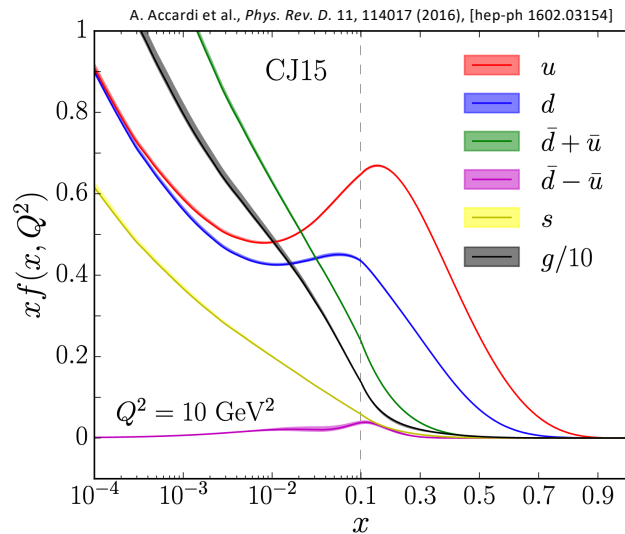


# Parton Distribution Functions



Wigner Function,  $\rho(x, \vec{k}_T, \vec{b}_T)$ :  
Full phase space parton distribution of the nucleon

Generalized Transverse Momentum Distributions



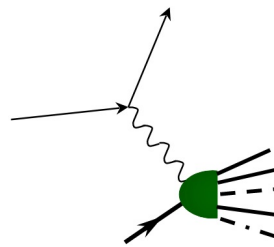
$$\int d^2 b_T$$

\* Deep Inelastic Scattering (DIS)

Transverse Momentum Distributions (TMDs)

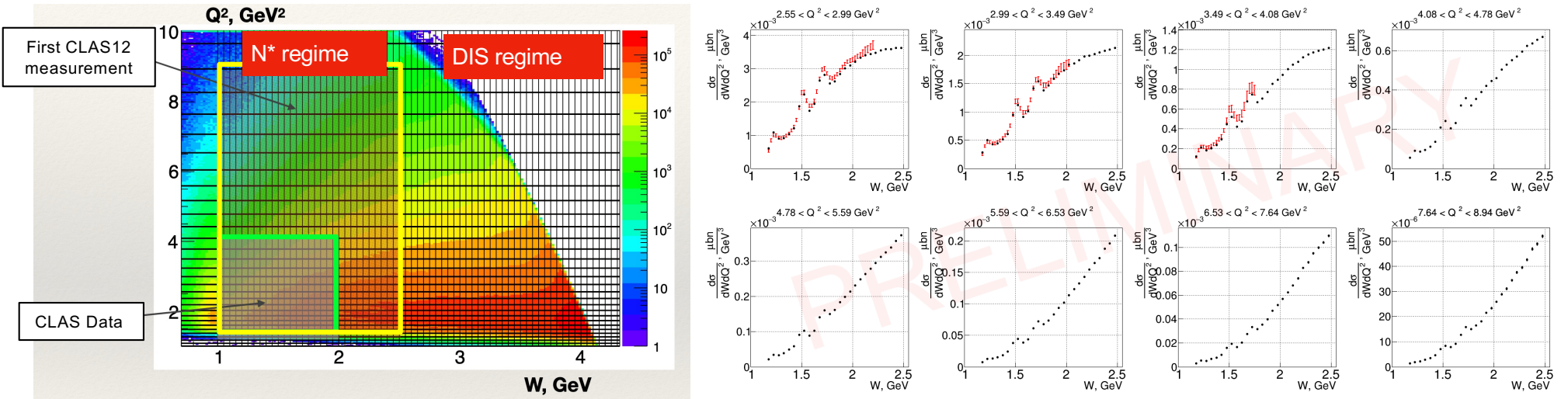
$$\int d^2 k_T$$

Parton Distribution Functions (PDFs)



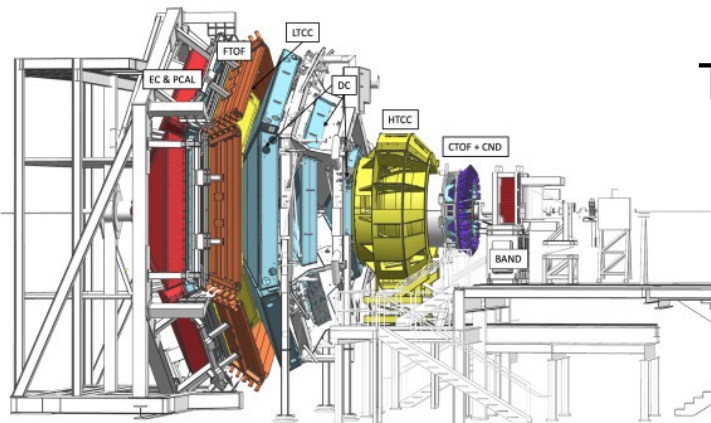
# Inclusive Electron Cross Section

- Preliminary results on inclusive electron scattering cross sections are available from CLAS12 in the kinematic range of  $1.18 < W < 2.50$  GeV and  $2.6 < Q^2 < 9.0$  GeV $^2$  and show agreement with world data in overlapping  $Q^2$  regions to within 20%.
- First data with broad coverage in  $W$  over the entire resonance region up to  $Q^2 = 9.0$  GeV $^2$  where the transition from quark-gluon confinement toward pQCD is expected to take place.
- Inclusive electron scattering data from CLAS12 and the evaluated resonant/non-resonant contributions will be important in order to gain insight into the ground state nucleon PDF at large values of  $x$  in the resonance region.



# Conclusions

- CLAS12 at JLab is ideally suited for a wide range of studies sensitive to nucleonic structure due to its high luminosity and nearly  $4\pi$  coverage.
- Three publications in the first year with unpolarized  $H_2$  data, two of which produced first time measurements.
- Entering the second phase of running with many different measurements (asymmetries and cross sections), different energies, different targets, etc.



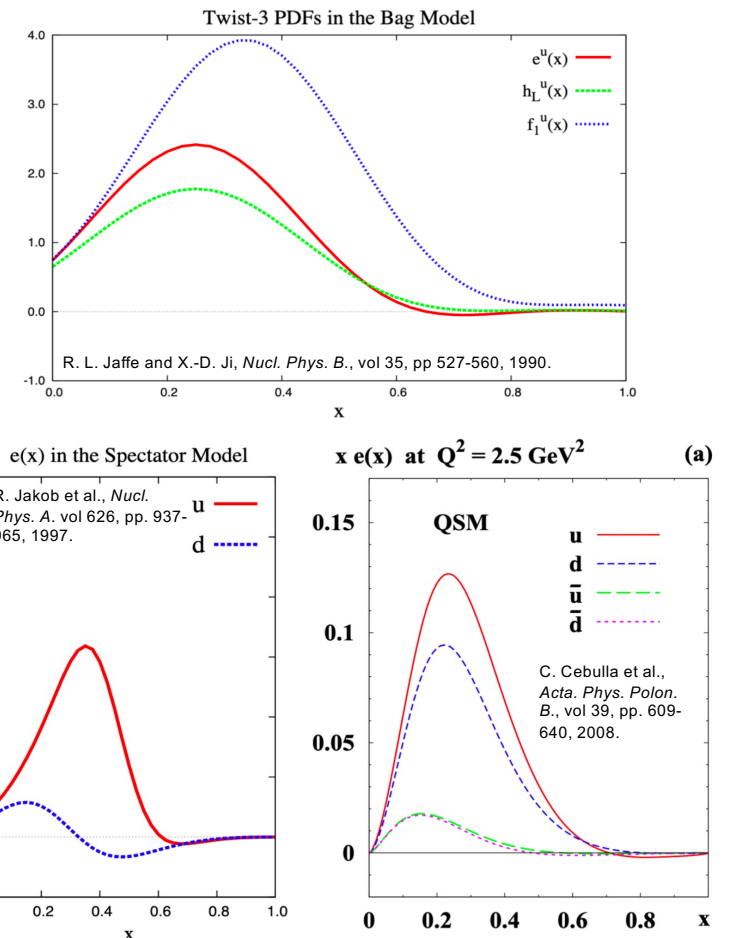
Thank you!



- Backup

# Twist-3 TMD/PDF $e(x)$

- Insight into largely unexplored quark-gluon correlations.
- $\int e(x)dx \rightarrow$  related to the strangeness content of the nucleon and the contributions from finite quark masses.
- $\int x e(x)dx \rightarrow$  proportional to the number of valence quarks in the nucleus.
- $\int x^2 e(x)dx \rightarrow \perp$  force on  $\perp$  polarized quarks in a unpolarized nucleon (similar to Boer-Mulders)
- Although the PDF  $e(x)$  has been studied extensively in models, direct experimental access has remained relatively scarce.



# Access to a rich phenomenology

**m = +2**

**Twist 2:**  $\sin(2\phi_h - 2\phi_{R_\perp}) \longrightarrow f_1(x) \otimes G_{1,TT}^\perp$

**Twist 3:**  $\sin(-\phi_h + 2\phi_{R_\perp}) \longrightarrow e(x) \otimes H_{1,TT}^\triangleleft$

**m = +1**

**Twist 2:**  $\sin(\phi_h - \phi_{R_\perp}) \longrightarrow f_1(x) \otimes (G_{1,OT}^\perp + G_{1,LT}^\perp)$

**Twist 3:**  $\sin \phi_{R_\perp} \longrightarrow e(x) \otimes (H_{1,OT}^\triangleleft + H_{1,LT}^\triangleleft)$

**m = 0**

Twist 2: n/a

**Twist 3:**  $\sin \phi_h \longrightarrow e(x) \otimes (H_{1,OO}^\perp + H_{1,OL}^\perp + H_{1,LL}^\perp)$

**m = -1**

Twist 2: cf m=+1

**Twist 3:**  $\sin(2\phi_h - \phi_{R_\perp}) \longrightarrow e(x) \otimes (H_{1,OT}^\perp + H_{1,LT}^\perp)$

**m = -2**

Twist 2: cf m=+2

**Twist 3:**  $\sin(3\phi_h - 2\phi_{R_\perp}) \longrightarrow e(x) \otimes H_{1,TT}^\perp$

# Polarized target measurements

$$F_{LU}^{\sin \phi_{R\perp}} = -x \frac{\vec{R} \sin \theta}{Q} \left[ \frac{M}{M_h} x e^q(x) H_1^{\triangleleft q}(z, \cos \theta, M_h) + \frac{1}{z} f_1^q(x) \tilde{G}(z, \cos \theta, M_h) \right]$$

“Interference Fragmentation Function”

A. Bacchetta and M. Radici, *Phys Rev D*, 67, 094002, (2003); hep-ph/021300

- Magnitude of  $\tilde{G}$  is significantly smaller than  $H_1^{\triangleleft}$  in model calculations.
- Ratio of  $A_{LU}/A_{UL}$  measurement should not depend on  $z$  or the pair mass if the contributions from  $\tilde{G}$  are negligible.

$$A_{LU} \propto x e^q(x) H_1^{\triangleleft}(z, M_h^2) + \frac{M_h}{zM} f_1^q(x) \tilde{G}(z, M_h^2)$$

$$A_{UL} \propto x h_L^q(x) H_1^{\triangleleft}(z, M_h^2) + \frac{M_h}{zM} g_1^q(x) \tilde{G}(z, M_h^2)$$

- Ultimately a problem for theorists... the measurement is required in order to access  $e(x)$  in either case.

# Potential Ambiguities

$$\begin{aligned}
 \frac{d\sigma^{\text{TFR}}}{dx_B dy d\zeta d^2\mathbf{P}_{h\perp} d\phi_S} = & \frac{2\alpha_{\text{em}}^2}{Q^2 y} \left\{ \left( 1 - y + \frac{y^2}{2} \right) \right. \\
 & \times \sum_a e_a^2 \left[ \hat{u}_1(x_B, \zeta, \mathbf{P}_{h\perp}^2) - |\mathbf{S}_\perp| \frac{|\mathbf{P}_{h\perp}|}{m_h} \hat{u}_{1T}^\perp(x_B, \zeta, \mathbf{P}_{h\perp}^2) \right. \boxed{\sin(\phi_h - \phi_S)} \\
 & + \lambda_l y \left( 1 - \frac{y}{2} \right) \sum_a e_a^2 \left[ S_\parallel \hat{l}_{1L}(x_B, \zeta, \mathbf{P}_{h\perp}^2) \right. \\
 & \left. \left. + |\mathbf{S}_\perp| \frac{|\mathbf{P}_{h\perp}|}{m_h} \hat{l}_{1T}^\perp(x_B, \zeta, \mathbf{P}_{h\perp}^2) \right] \cos(\phi_h - \phi_S) \right\}.
 \end{aligned}$$

M. Anselmino et al., Phys. Lett. B. 699 (2011), 108-118, [hep-ph] 1102.4214

The same azimuthal asymmetries can appear in both the CFR and TFR complicating their interpretation...



$$[F_{UT,T}^{\sin(\phi_h - \phi_S)}]_{\text{TFR}} = - \sum_a e_a^2 x_B \frac{|\mathbf{P}_{h\perp}|}{m_h} \hat{u}_{1T}^\perp(x_B, \zeta, \mathbf{P}_{h\perp}^2)$$

$$[F_{UT,T}^{\sin(\phi_h - \phi_S)}]_{\text{CFR}} = \mathcal{C} \left[ - \frac{\hat{\mathbf{h}} \cdot \mathbf{k}_\perp}{m_N} f_{1T}^\perp D_1 \right]$$

$$[F_{LT}^{\cos(\phi_h - \phi_S)}]_{\text{TFR}} = \sum_a e_a^2 x_B \frac{|\mathbf{P}_{h\perp}|}{m_h} \hat{l}_{1T}^\perp(x_B, \zeta, \mathbf{P}_{h\perp}^2)$$

$$[F_{LT}^{\cos(\phi_h - \phi_S)}]_{\text{CFR}} = \mathcal{C} \left[ \frac{\hat{\mathbf{h}} \cdot \mathbf{k}_\perp}{m_N} g_{1T} D_1 \right]$$

... six more azimuthal asymmetries appear in the CFR at leading twist which are absent in the TFR.

# Categorizing Fracture Functions

- At leading twist fracture functions exist that can be organized into tables of quark and nucleon polarizations just like the more familiar PDFs.
- Access to *both*  $k_T$  and  $p_T$  effects gives  $2 \times 8 = 16$  FrFs.

The diagram illustrates the categorization of fracture functions (FrFs) based on quark and nucleon polarizations. It features two tables, each with three columns corresponding to Quark polarization (U, L, T) and three rows corresponding to Nucleon polarization (U, L, T). The left table represents the initial state, and the right table represents the final state. Double-headed arrows between the tables are labeled 'CFR' (Conformal Flavour Rotation) and 'TFR' (Transverse Flavour Rotation), indicating the symmetry of the categorization under these transformations.

| Quark polarization   |                |          |                     |
|----------------------|----------------|----------|---------------------|
|                      | U              | L        | T                   |
| Nucleon polarization | $f_1$          |          | $h_1^\perp$         |
|                      | $g_{1L}$       |          | $h_{1L}^\perp$      |
|                      | $f_{1T}^\perp$ | $g_{1T}$ | $h_1, h_{1T}^\perp$ |

| Quark polarization   |                                      |                                      |  |
|----------------------|--------------------------------------|--------------------------------------|--|
|                      | U                                    | L                                    | T  |
| Nucleon polarization | $\hat{u}_1$                          | $\hat{l}_1^{\perp h}$                | $\hat{t}_1^h, \hat{t}_1^\perp$   |
|                      | $\hat{u}_{1L}^{\perp h}$             | $\hat{l}_{1L}$                       | $\hat{t}_{1L}^h, \hat{t}_{1L}^\perp$   |
|                      | $\hat{u}_{1T}^h, \hat{u}_{1T}^\perp$ | $\hat{l}_{1T}^h, \hat{l}_{1T}^\perp$ | $\hat{t}_{1T}^h, \hat{t}_{1T}^{hh}$<br>$\hat{t}_{1T}^{\perp\perp}, \hat{t}_{1T}^{\perp h}$ |

M. Anselmino et al., Phys. Lett. B, 706 (2011), 46–52, [hep-ph] 1109.1132

# Analogs to PDFs

- A direct relationship exists to the eight leading twist PDFs after the fracture functions are integrated over the fractional longitudinal nucleon momentum.

$$z(1 - x) = \boxed{E_h/E = \zeta}$$

$$\sum_h \int d\zeta M_a(x_B)(x_B, k_\perp^2, \zeta) = (1 - x_B) f_a(x_B, k_\perp^2)$$

M. Anselmino et al., Phys. Lett. B. 699 (2011), 108, [hep-ph] 1102.4214

|                      |   | Quark polarization |          |                     |
|----------------------|---|--------------------|----------|---------------------|
|                      |   | U                  | L        | T                   |
| Nucleon polarization | U | $f_1$              |          | $h_1^\perp$         |
|                      | L |                    | $g_{1L}$ | $h_{1L}^\perp$      |
|                      | T | $f_{1T}^\perp$     | $g_{1T}$ | $h_1, h_{1T}^\perp$ |

Boer-Mulders analog

etc. etc.

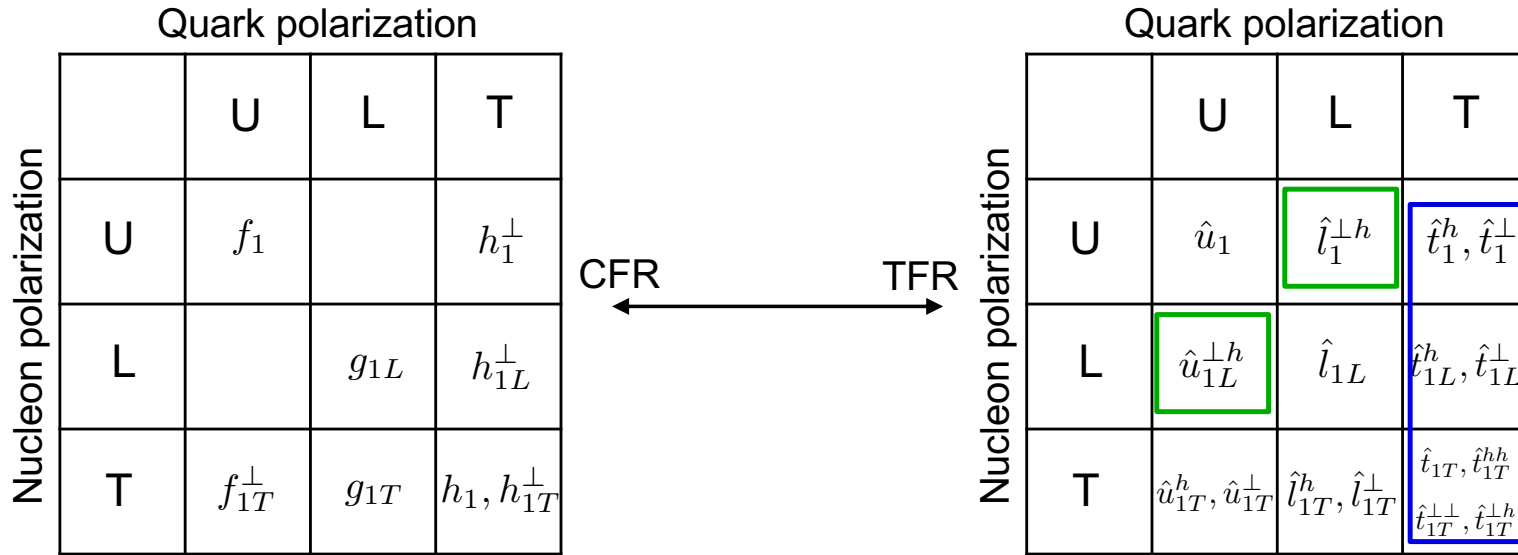
Sivers analog

|                      |   | Quark polarization                   |                                      |  |
|----------------------|---|--------------------------------------|--------------------------------------|--|
|                      |   | U                                    | L                                    | T  |
| Nucleon polarization | U | $\hat{u}_1$                          | $\hat{l}_1^{\perp h}$                | $\hat{t}_1^h, \hat{t}_1^\perp$   |
|                      | L | $\hat{u}_{1L}^{\perp h}$             | $\hat{l}_{1L}$                       | $\hat{t}_{1L}^h, \hat{t}_{1L}^\perp$   |
|                      | T | $\hat{u}_{1T}^h, \hat{u}_{1T}^\perp$ | $\hat{l}_{1T}^h, \hat{l}_{1T}^\perp$ | $\hat{t}_{1T}, \hat{t}_{1T}^{hh}$<br>$\hat{t}_{1T}^{\perp\perp}, \hat{t}_{1T}^{\perp h}$ |

M. Anselmino et al., Phys. Lett. B. 706 (2011), 46-52, [hep-ph] 1109.1132

# Single hadron limitations

- FrFs describing transversely polarized quarks are chiral odd and inaccessible in TFR single hadron production where there is no access to a chiral odd FF.
- Functions with double superscripts containing  $h$  and  $\perp$  have give the unique possibility of measuring longitudinal polarized quarks in unpolarized nucleons (and vice versa) but disappear after integration over either momentum.



M. Anselmino et al., Phys. Lett. B, 706 (2011), 46-52, [hep-ph] 1109.1132

# Extension to (collinear) twist-3

- Twist-3 fracture functions defined through quark-quark, quark-gluon and pure gluonic correlators.

$$\begin{aligned} & \int \frac{d\lambda}{2\pi} e^{-ix\lambda P^+} \sum_X \langle h_A | \bar{\psi}_j(\lambda n) \mathcal{L}_n^\dagger(\lambda n) | h_B(P_h), X \rangle \langle X, h_B(P_h) | \mathcal{L}_n(0) \psi_i(0) | h_A \rangle \Big|_{\text{twist-3, } U,L-\text{target}} \\ &= \frac{1}{2N_c P^+} \left[ (\gamma_\perp \cdot P_{h\perp})_{ij} \hat{u}_2^{\perp h}(x, \xi, P_{h\perp}) + (\gamma_5 \gamma_\perp \cdot \tilde{P}_{h\perp})_{ij} \hat{l}_2^{\perp h}(x, \xi, P_{h\perp}) \right] \\ &+ \frac{S_L}{2N_c P^+} \left[ (\gamma_\perp \cdot \tilde{P}_{h\perp})_{ij} \hat{u}_{2L}^{\perp h}(x, \xi, P_{h\perp}) + (\gamma_5 \gamma_\perp \cdot P_{h\perp})_{ij} \hat{l}_{2L}^{\perp h}(x, \xi, P_{h\perp}) \right] + \dots, \end{aligned}$$

K.B. Chen, J.B. Ma, X.B. Tong (Private correspondence)  
c.f. JHEP, vol 11 (2021), [hep-ph] 2108.13582

Additional contributions from quark and quark-gluon correlators with transverse momentum derivatives...

| N \ q | U                                    | L                                    | T   |
|-------|--------------------------------------|--------------------------------------|---|
| U     | $\hat{u}_1$                          | $\hat{l}_1^{\perp h}$                | $\hat{t}_1^h, \hat{t}_1^\perp$  |
| L     | $\hat{u}_{1L}^{\perp h}$             | $\hat{l}_{1L}$                       | $\hat{t}_{1L}^h, \hat{t}_{1L}^\perp$  |
| T     | $\hat{u}_{1T}^h, \hat{u}_{1T}^\perp$ | $\hat{l}_{1T}^h, \hat{l}_{1T}^\perp$ | $\hat{t}_{1T}^h, \hat{t}_{1T}^\perp, \hat{t}_{1T}^{\perp\perp}, \hat{t}_{1T}^{\perp h}$ |

Twist-2

Already accessible with data collected at CLAS12.

| N \ q | U  | L                                       | T  |
|-------|--|---|--|
| U     | $\tilde{u}_2^{\perp h}$                          | $\tilde{l}_2^{\perp h}$                 | $\tilde{t}_2, \tilde{e}_2$   |
| L     | $\tilde{u}_{2L}^{\perp h}$                       | $\tilde{l}_{2L}^{\perp h}$              | $\tilde{t}_{2L}, \tilde{e}_{2L}$   |
| T     | $\tilde{u}_{2T}^{\perp h}, \tilde{u}_{2T}^\perp$ | $\tilde{l}_T, \tilde{l}_{2T}^{\perp h}$ | $\tilde{t}_{2T}^h, \tilde{e}_{2T}^h, \tilde{t}_{2T}^{\perp h}, \tilde{e}_{2T}^{\perp h}$ |

Collinear twist-3

# Twist-3 Observables

$$\begin{aligned}
& \int \frac{d\lambda}{2\pi} e^{-ix\lambda P^+} \sum_X \left\langle h_A \left| \bar{\psi}_j(\lambda n) \mathcal{L}_n^\dagger(\lambda n) |h_B(P_h), X\rangle \langle X, h_B(P_h)| \mathcal{L}_n(0) \psi_i(0) \right| h_A \right\rangle \Big|_{\text{twist-3, } U,L-\text{target}} \\
&= \frac{1}{2N_c P^+} \left[ (\gamma_\perp \cdot P_{h\perp})_{ij} \hat{u}_2^{\perp h}(x, \xi, P_{h\perp}) + (\gamma_5 \gamma_\perp \cdot \tilde{P}_{h\perp})_{ij} \hat{l}_2^{\perp h}(x, \xi, P_{h\perp}) \right] \\
&\quad + \frac{S_L}{2N_c P^+} \left[ (\gamma_\perp \cdot \tilde{P}_{h\perp})_{ij} \hat{u}_{2L}^{\perp h}(x, \xi, P_{h\perp}) + (\gamma_5 \gamma_\perp \cdot P_{h\perp})_{ij} \hat{l}_{2L}^{\perp h}(x, \xi, P_{h\perp}) \right] + \dots,
\end{aligned}$$

K.B. Chen, J.B. Ma, X.B. Tong (Private correspondence)  
c.f. JHEP, vol 11 (2021), [hep-ph] 2108.13582

Target-spin Asymmetry

$$A_{UL} \propto S_L \sqrt{2\epsilon(1+\epsilon^2)} F_{UL}^{\sin \phi_h} \sin \phi_h$$

$F_{UU}^{\cos \phi_h} \sim \tilde{u}_2^{\perp h} + \dots, \quad F_{LU}^{\sin \phi_h} \sim \tilde{l}_2^{\perp h} + \dots, \quad F_{UL}^{\sin \phi_h} \sim \tilde{u}_{2L}^{\perp h} + \dots, \quad F_{LL}^{\cos \phi_h} \sim \tilde{l}_{2L}^{\perp h} + \dots$

Beam-spin Asymmetry

$$A_{LU} \propto S_L \sqrt{2\epsilon(1-\epsilon^2)} F_{LU}^{\sin \phi_h} \sin \phi_h$$

$$\frac{d\sigma}{dxdydzdP_T^2 d\phi_h} = \hat{\sigma}_U \left[ F_{UU,T} + \varepsilon F_{UU,L} + \sqrt{2\varepsilon(1+\varepsilon)} F_{UU}^{\cos \phi_h} \cos \phi_h + \varepsilon F_{UU}^{\cos 2\phi_h} \cos(2\phi_h) + \lambda_\ell \sqrt{2\varepsilon(1-\varepsilon)} F_{LU}^{\sin \phi_h} \sin \phi_h + S_L \sqrt{2\varepsilon(1+\varepsilon)} F_{UL}^{\sin \phi_h} \sin \phi_h + \lambda_\ell S_L \sqrt{1-\varepsilon^2} F_{LL} + \lambda_\ell S_L \sqrt{2\varepsilon(1-\varepsilon)} F_{LL}^{\cos \phi_h} \cos \phi_h + S_L \varepsilon F_{UL}^{\sin 2\phi_h} \sin(2\phi_h) \right]$$

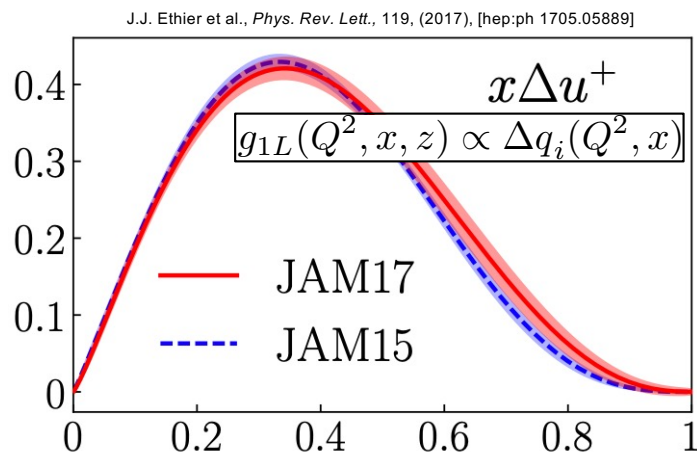
In the TFR the  $\sin(2\phi)$  and  $\cos(2\phi)$  modulations appear at twist-4 because there are no appropriate FrFs to generate the correct tensor structure.

# A<sub>LL</sub> – The Best of Both Worlds

$$\frac{d\sigma}{dxdydzdP_T^2} = 2\pi\hat{\sigma}_U \sum_q e_q^2 \left[ F_{UU,T} + \lambda S_L \sqrt{1-\varepsilon^2} F_{LL} \right]$$

M. Anselmino et al., Phys. Lett. B, 699 (2011), 108, [hep-ph] 1102.4214

At leading twist for the case of a longitudinally polarized target and a single hadron produced in the TFR, only two terms appear:



J.J. Ethier et al., Phys. Rev. Lett., 119, (2017), [hep-ph 1705.05889]

$$F_{UU,T} \propto \tilde{u}_1(x, \zeta, P_T^2) = \int d^2 k_T \hat{u}_1$$

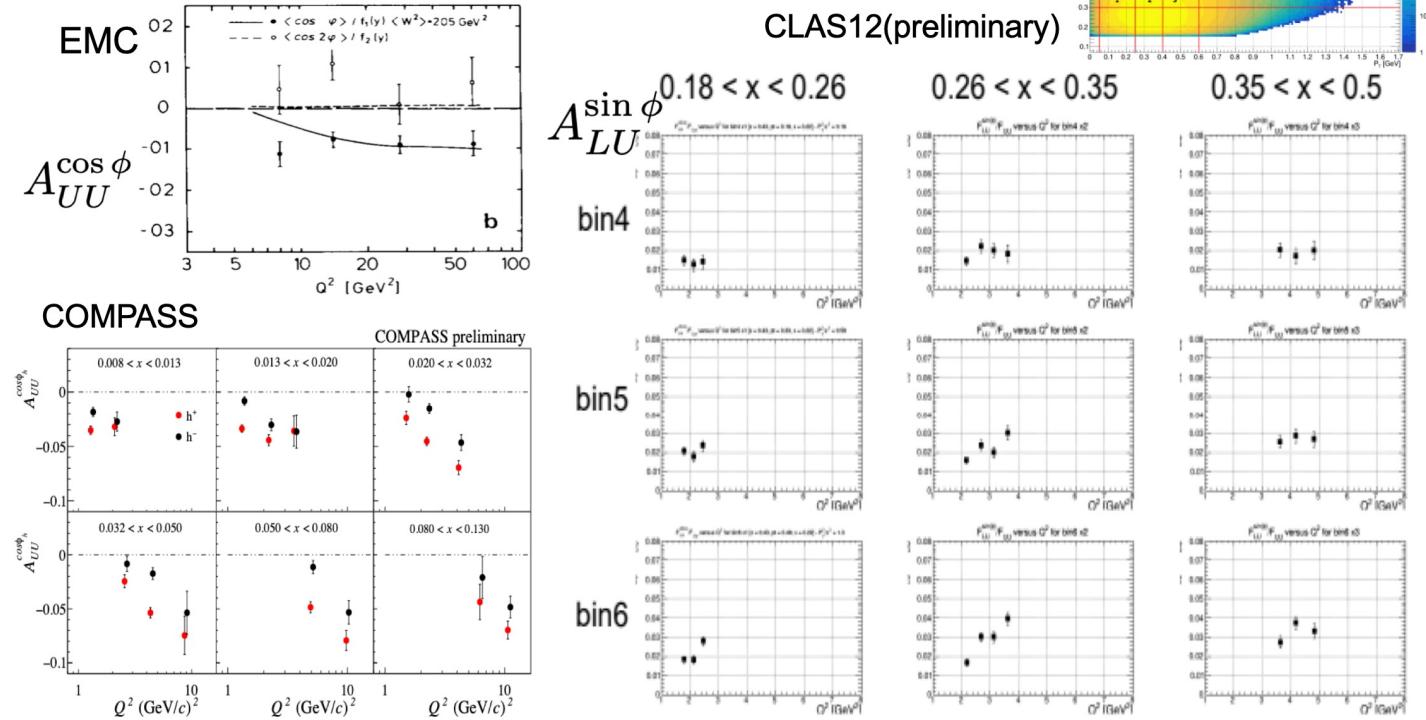
$$F_{LL} \propto \tilde{l}_{1L}(x, \zeta, P_T^2) = \int d^2 k_T \hat{l}_{1L}$$

**Double Spin Asymmetry:**  $A_{LL} = \lambda_\ell S_L \frac{\sqrt{1-\varepsilon^2} F_{LL}}{F_{UU,T}}$

1. Single hadron → Highest statistics
2. Leading twist → Simple interpretation
3. Linked to  $g_1$  → easiest test of FrF prediction

$$\sum_h \int \zeta d\zeta \int d^2 P_T \hat{l}_{1L} = (1-x) g_{1L}(x, k_T^2)$$

## Attempts to understand $Q^2$ -dependence of HT

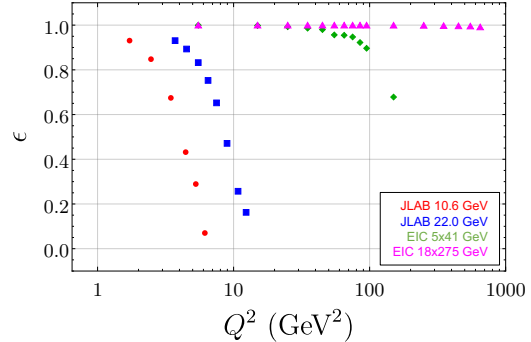


The ratios of SFs (to  $F_{UU}$ ) are not decreasing with  $Q$ !!!

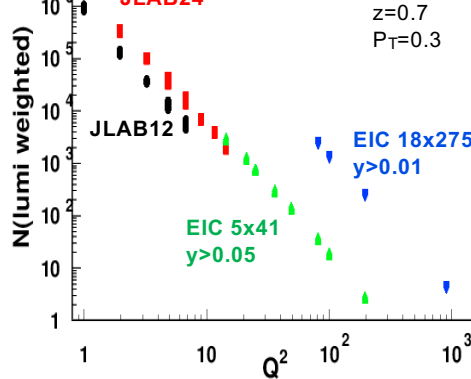
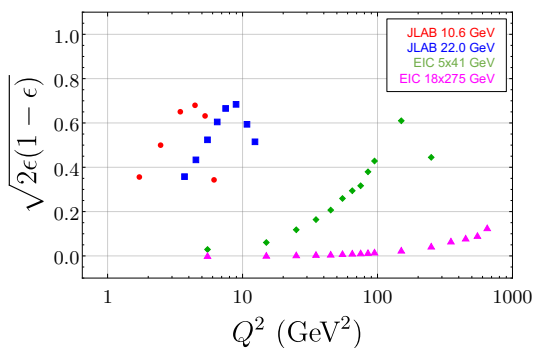
The HT observables, don't look much like HT observables, something missing in understanding  
Understanding of these behavior can be a key to understanding of other inconsistencies

# Kinematic Suppression at EIC

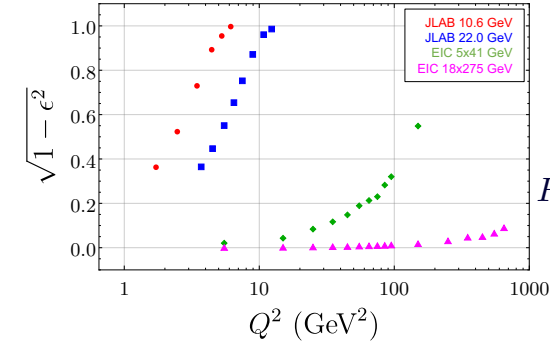
$F_{UU,L}$   
 $F_{UU}^{\cos 2\phi}$   
 $F_{UT}^{(3\phi - \phi_S)}$   
 $F_{UT,L}^{\sin(\phi - \phi_S)}$   
etc



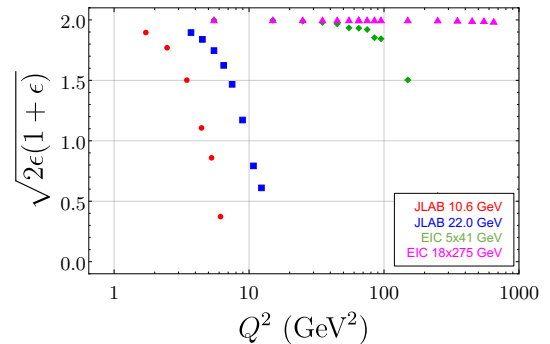
$F_{LU}^{\sin \phi}$   
 $F_{LU}^{\sin \phi_{R_\perp}}$   
 $F_{LL}^{\cos \phi}$   
etc



At the premier EIC luminosity of 10x275 many observables are **heavily suppressed**.



$F_{LL}$   
 $F_{LU}^{\sin \Delta \phi}$   
 $F_{LU}^{\sin(\phi_h - \phi_{R_\perp})}$   
etc



$F_{UL}^{\sin \phi}$   
 $F_{UU}^{\cos \phi}$   
 $F_{UT}^{\sin \phi_S}$   
 $F_{UT}^{\sin \phi_S}$   
etc